Description and Performance of a Fiber-Optic Confocal Fluorescence Spectrometer

REBECCA RICHARDS-KORTUM,* ANTHONY DURKIN, and JING ZENG

Biomedical Engineering Program, Department of Electrical and Computer Engineering, University of Texas at Austin, Austin, Texas 78712

We describe a fiber-optic-based confocal fluorescence spectrometer for obtaining depth-resolved, attenuated fluorescence emission spectra with lateral resolution of several microns and depth resolution of tens of microns. The confocal optics of the spectrometer are small, inexpensive, and easy to construct and to interface to existing spectrometers. We compare the performance of this system to that of conventional fluorescence spectrometers for nonscattering homogeneous and inhomogeneous samples. We demonstrate that the confocal measurements readily provide information about the sample geometry and optical properties not available from nonconfocal measurements. Potential applications of the technique are discussed.

Index Headings: **Fluorescence spectroscopy; Confocal; Fiber optic.**

INTRODUCTION

Many studies have demonstrated that fluorescence spectroscopy can provide information about the chemical composition of human tissue which is useful in the detection of pathology.[1-6] Fluorescence spectra can be obtained *in vivo* in near real time with the use of fiber-optic catheters often introduced through the biopsy channel of standard endoscopes.[3,4] The potential clinical advantages of the proposed "optical biopsy" techniques are clear; diagnostic and prognostic information usually obtained from histologic examination of a biopsy can be inferred instead by analyzing optical spectra obtained without the need for tissue removal. Several two-dimensional spectroscopic imaging systems designed to implement this concept clinically have been proposed and tested.[5,6] These systems record fluorescence intensities at several emission wavelengths sequentially from the surface of tissue; ratios of images at various wavelength combinations produce an image indicating tissue pathology.

Although the nonconfocal optical techniques proposed to date provide a sensitive measure of the chromophores present in tissue and their relative contribution to the fluorescence exiting the tissue surface, such measurements provide little quantitative information about the variation in chromophore concentration as a function of depth beneath the surface. Assessing the physical organization of tissue composition with depth is important in many diagnostic decisions; for example, epithelial precancers and cancers are differentiated and graded on the basis of the portion of the epithelium and supporting stroma containing neoplastic cells.[7] In a nonconfocal fluorescence measurement from a layered sample, homogeneous in the lateral directions, the relationship between the physical organization of chromophores and fluorescence intensity measured from the tissue surface ($S_{\text{nonconfocal}}(\lambda_x, \lambda_m)$) as a function of excitation (λ_x) and emission wavelength (λ_m) can be described mathematically as in Eq. 1:[8]

$$S_{\text{nonconfocal}}(\lambda_x, \lambda_m) = I_0 \int_0^L dz\, H_{\text{in}}(z, \lambda_x) S_{\text{int}}(z, \lambda_x, \lambda_m) H_{\text{out}}(z, \lambda_m). \quad (1)$$

Here, $S_{\text{int}}(z, \lambda_x, \lambda_m)$ represents the intrinsic fluorescence per unit thickness of the sample layer located at depth z from the surface, $H_{\text{in}}(z, \lambda_x)$ represents the fraction of incident intensity (I_0) reaching the layer at z, $H_{\text{out}}(z, \lambda_m)$ represents the fraction of fluorescence from the layer exiting the tissue surface, and L is the sample thickness. Thus, the fluorescence measured from the surface can be viewed as a weighted average of the contributions from each layer within the penetration depth of the excitation light, with the weighting determined by the intrinsic fluorescence, the tissue organization, and the tissue attenuation. Several techniques to deconvolve the intrinsic fluorescence information from surface measurements of fluorescence and reflectance have been presented;[9,10] however, they are applicable only to homogeneous samples.

Although proposed nonconfocal spectroscopic measurements[1-6] provide limited information about the depth distribution of chromophores, confocal microscopy provides detailed images of tissue structure from various layers within a sample without the need for physical sectioning.[11] In a confocal microscope, excitation light is focused onto a small spot within the sample; light originating at the in-focus point is imaged onto a detector, where a small pinhole is used to reject light from other planes within the sample.[11] Three-dimensional images of scattering media with submicron lateral and axial resolution are routinely achieved with the use of scanning confocal microscopes with high-numerical-aperture objectives. Several groups have presented designs for confocal microscopes based on single-mode optical fibers.[12-15]

Confocal fluorescence images are generally produced by measuring the emission intensity as a function of position over a single, wide-emission-bandwidth region. However, the confocal concept can clearly be extended to obtain depth-resolved spectra. Confocal microscopes have been modified to obtain Raman spectra confocally from the nucleus and cytoplasm of single living cells.[16,17] Steady-state and time-resolved fluorescence spectra with three-dimensional resolution have been reported with the use of a spectrometer coupled to a confocal microscope.[18] Spectra obtained from thin liquid films and small latex particles containing fluorophores have been used to estimate fluorophore concentrations and sample dimen-

Received 21 September 1993; revision received 3 December 1993.
* Author to whom correspondence should be sent.

0003-7028/94/4803-0350$2.00/0

sions.[18] Because the confocal technique rejects signal from out-of-focus points, the technique can potentially be used even in the presence of scattering or absorbing impurities. This can easily be seen by examining the dependence of the confocal signal on the distance between the sample surface and the in-focus point, z (Eq. 2):[19]

$$S_{CF}(z, \lambda_x, \lambda_m) = I_0 H'_{in}(z, \lambda_x) S_{int}(z, \lambda_x, \lambda_m) H'_{out}(z, \lambda_m) \Delta. \quad (2)$$

Here, $S_{int}(z, \lambda_x, \lambda_m)$ represents the same intrinsic fluorescence intensity per unit thickness of the sample at depth z, $H'_{in}(z, \lambda_x)$ represents the fraction of the excitation intensity (I_0) reaching the in-focus spot, $H'_{out}(z, \lambda_m)$ is the fraction of emission intensity passing through the confocal pinhole, and Δ is the axial resolution of the confocal system (assumed to be small in comparison to the inverse of the total attenuation coefficient). Thus, by profiling the confocal spectra as a function of depth, the product of the sample attenuation at the excitation and emission wavelengths and the intrinsic fluorescence (depth-resolved, attenuated-fluorescence spectra) can be recorded.

Although spectrometers based on confocal microscopes provide measurements of depth-resolved attenuated fluorescence, confocal microscopes are large and relatively expensive, making potential *in vivo* use difficult. In this paper, we describe a fiber-optic-based confocal fluorescence spectrometer for obtaining depth-resolved, attenuated-fluorescence emission spectra with lateral resolution of several microns and depth resolution of tens of microns. This spectrometer is small, inexpensive, and easy to construct and to interface to existing spectrometers. We compare the performance of this fiber-optic system to that of conventional fluorescence spectroscopy for nonscattering homogeneous and inhomogeneous samples. Finally, we discuss potential applications of this technology.

METHODS

Figure 1 shows a block diagram of the fiber-optic confocal spectrometer. The heart of the system is a single-mode, 2 × 2 fiber-optic bi-directional coupler (Aster) with 6 μm field mode diameter and 0.11 numerical aperture (NA). Excitation light at 488 nm was provided by coupling light from a continuous-wave argon-ion laser (Coherent Innova 100) into one of the proximal legs of the bi-directional coupler. A power meter monitored the excitation light exiting one of the distal legs of the coupler. Excitation light exiting the other distal leg was directed onto the sample via two microscope objectives; a 0.2 NA 10× objective collimated light exiting the fiber, and a 20×, 0.4 NA, long-working-distance objective was used to refocus the excitation light onto the sample. The beam profile was measured at various points along the optical axis near the focal plane of the 20× microscope objective by the use of the knife-edge method.[20] Fluorescence from the sample was collected with the same microscope objectives; the finite diameter of the fiber optic served as the effective confocal pinhole. Fluorescence exiting the free proximal leg of the bi-directional coupler was focused onto the 1-mm entrance slit of a polychromator (Jarrell Ash Monospec 18) coupled to an intensified diode array (Princeton Instruments IRY600G/RB). A long-pass filter

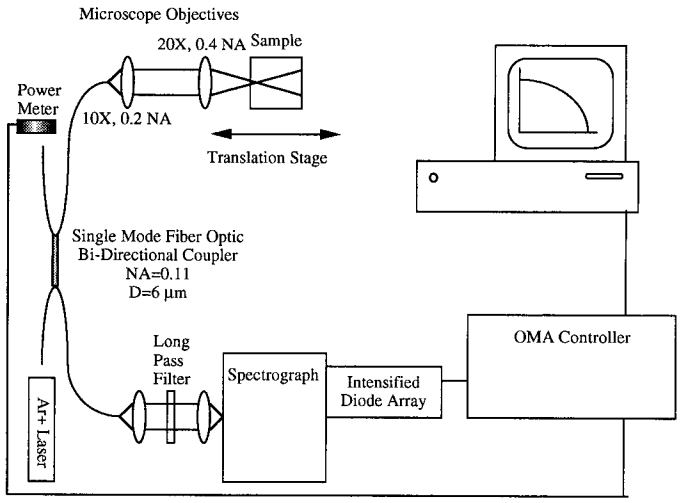

FIG. 1. Block diagram of the fiber-optic confocal spectrometer.

was used to reject scattered excitation light at the spectrometer.

The diode array controller (Princeton Instruments ST-121) recorded fluorescence intensity as a function of diode number and the output voltage from the power meter simultaneously; all fluorescence intensities are reported relative to excitation power, in arbitrary units. Wavelength calibration was accomplished with the use of the 488-nm excitation line and two HeNe lines at 543.5 and 632.8 nm. System spectral response was measured from the width of these lines. Data obtained with this system were corrected for the nonuniform spectral response of the detection system by calibration with an NIST traceable tungsten ribbon filament lamp (Optronics Model 550C). In the acquisition of the correction factors, the lamp was inserted in place of the sample, and a spectrum of the lamp was recorded. Thus, the correction factors include the wavelength-dependent spectral response of both the diode array detector and the spectrograph and the wavelength dependence of the split ratio of the fiber-optic coupler. Correction factors were smoothed with the use of a five-pixel-wide (3-nm-wide) averaging filter prior to application to data. Thus, nonuniformities in the diode-to-diode sensitivity of the detector below the system spectral resolution were not corrected by this procedure.

Fluorescent samples to be investigated were mounted on a translation stage with 10-μm resolution. Fluorescence spectra were measured as the sample was translated along the optical axis, so that the focal point of the optical system passed through the surface and into the sample. Excitation powers incident on the sample front face varied from 10 to 40 μW; fluorescence signal was integrated for 1 s at each point. Measurements were repeated 1–10 times at each point, and results were averaged. No evidence of photobleaching was observed. Dark current was recorded by replacing the sample with a blank cuvette and repeating the measurement. Dark current was subtracted from all data, and the zero on the fluorescence intensity scale represents the point at which no signal was detected above dark current.

To characterize the depth resolution of the system, we made confocal measurements from a very thin fluorescent sample. This was produced by placing a thin layer of

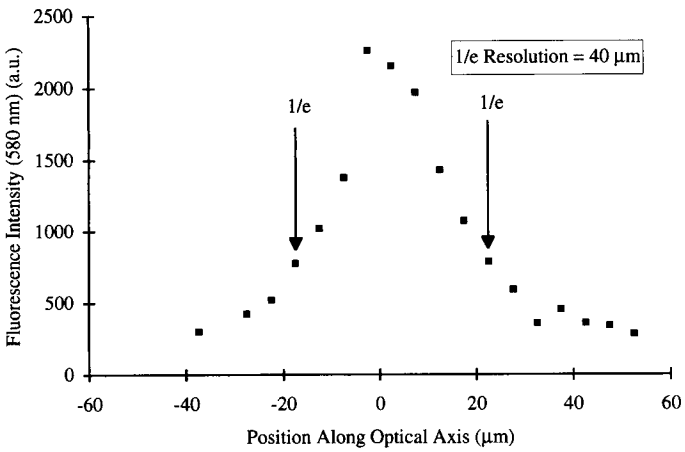

FIG. 2. Peak fluorescence intensity recorded from a thin film of Rhodamine 6G dye as the sample was translated along the optical axis. The axial resolution of the confocal spectrometer, estimated from the $1/e$ width of this peak, is 40 μm.

Rhodamine 6G dye in ethylene glycol (8 g/L) on a microscope slide. The solvent was allowed to evaporate, leaving a thin film of Rhodamine 6G on the slide. To characterize the behavior of the system for nonscattering materials, we made confocal measurements from both inhomogeneous and homogeneous samples. The homogeneous sample consisted of a 300 μM solution of flavin adenine dinucleotide (FAD) (Kodak) in pH 7.4, isotonic phosphate-buffered saline (PBS) in a 1-cm-pathlength quartz cuvette. Finally, an inhomogeneous sample, consisting of two homogeneous layers, was examined. A 1.58-mm-thick layer containing 1 mg/L of Rhodamine 6G in gelatin (5.8 g Knox unflavored gelatin in 100 mL PBS) was placed over a 1.66-mm-thick layer containing 1.5 mM FAD in gelatin (5.8 g Knox unflavored gelatin in 100 mL PBS). Layers were separated by a thin sheet of plastic wrap to prevent dye diffusion between layers. The two-layer sample was placed inside a quartz cuvette, with light directly incident on the layer containing Rhodamine 6G. In each case, fluorescence spectra were obtained as the sample was translated along the optical axis so that the focal plane of the confocal spectrometer passed across the front surface and into the sample. Corresponding spectra were also obtained from PBS and gelatin blanks. The fluorescence of the blank was negligible in comparison to that of the sample of interest in all cases.

On-axis transmission spectra of the 300 μM FAD solution and the individual Rhodamine 6G and FAD gelatin layers were measured from 250 to 700 nm with the use of a double-beam absorption spectrophotometer (Hitachi UV3300). Absorption coefficients were calculated from the Beer–Lambert law. Nonconfocal fluorescence spectra of the individual Rhodamine 6G and FAD gelatin layers and the two-layer sample were measured with a conventional fluorescence spectrophotometer (Spex Fluorolog II) at 488-nm excitation.

RESULTS AND DISCUSSION

The spectral resolution of the confocal detection system was measured to be 6 nm FWHM. The lateral and the axial resolution of the confocal optics were estimated first from measurements of the excitation beam profile. The $1/e$ diameter of the focal spot was 3.6 μm; the depth of focus was 32 μm. A more precise estimate of the axial resolution of the confocal system is provided by the results of the experiments conducted with the thin film of Rhodamine 6G dye, shown in Fig. 2. The peak fluorescence intensity [in arbitrary units (a.u.)] is plotted as a function of the axial position of the sample. The maximum intensity occurs when the sample is at the focal plane of the system (axial position = 0.0 μm) and drops off on either side. The $1/e$ diameter of this peak is 40 μm; this value is similar to the depth of focus, as expected. It also agrees well with the predicted resolution for a confocal microscope operating at 578-nm emission with a 0.22 effective numerical aperture.[21]

To characterize the dependence of the confocal signal on the optical properties of a homogeneous sample, we obtained data from a nonscattering solution containing 300 μM FAD. Figure 3a shows the fluorescence spectra (in a.u.) obtained as the sample was translated along the optical axis. Figure 3b shows the intensity at 540 nm as a function of position along the optical axis for the same sample. The focal point was defined to be the position on the optical axis at which maximal fluorescence signal was detected. As the front face of the sample crossed the focal point of the system, the fluorescence intensity increased rapidly in a distance consistent with the axial resolution. The fluorescence intensity dropped more slowly as the focal point was translated deeper within the sample; however, the shape of the emission spectrum remained constant. This drop in intensity is due to attenuation of excitation and emitted light as predicted by Eq. 2. Figure 3c shows the absorption coefficient of this sample as a function of wavelength. At 488 nm, the sample is moderately absorbing; at the emission wavelengths, the sample is transparent. Thus, in this case, the detected confocal intensity drops due to the attenuation of excitation light; the shape of the emission spectrum remains constant with depth because the sample is transparent at all emission wavelengths. Assuming that H'_{in} and H'_{out} can be described by Beer's law, and that excitation and detected emitted light travel along the optical axis, the drop in fluorescence intensity with position along the optical axis should be given by Eq. 3:

$$S_{\text{CF}}(z, \lambda_x, \lambda_m) = I_0 e^{-\mu_a(\lambda_x)z} S_{\text{int}}(z, \lambda_x, \lambda_m) e^{-\mu_a(\lambda_m)z} \Delta \quad (3)$$

where the absorption coefficient is denoted by μ_a. Figure 3d compares the experimentally measured data at the peak emission wavelength to the predicted value of Eq. 3 with the use of measured values of the absorption coefficients at the excitation and peak emission wavelengths. The fluorescence intensity has been normalized to a maximum value of unity. Reasonable agreement is observed; however, the measured intensity falls off slightly more rapidly than the prediction. In Eq. 3, we have assumed that all excitation and detected emission light travels along the optical axis. Differences in measured and predicted values are likely due to the fact that the optical system has a finite numerical aperture.

The advantages of the confocal spectrometer are best illustrated in Fig. 4, which contrasts the fluorescence spectra of a two-layer, inhomogeneous, nonscattering sample recorded with the fiber-optic confocal spectrometer to spectra from a conventional, nonconfocal spectrometer.

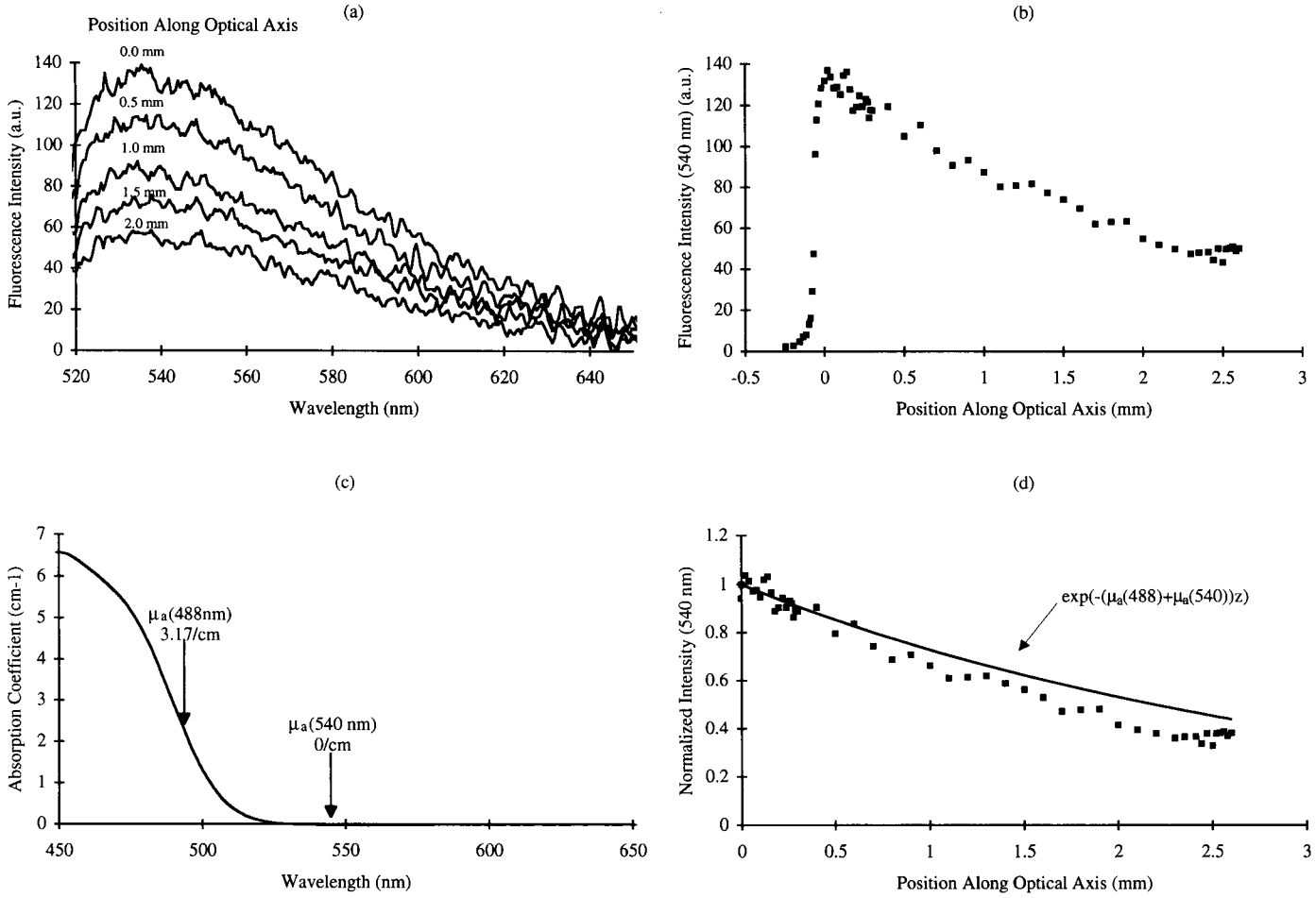

FIG. 3. (**a**) Fluorescence emission spectra of 300 μM FAD recorded when the sample front face was at the focal point of the confocal system (relative position along the optical axis = 0 μm), and as the focal point was translated deeper within the sample. (**b**) Peak fluorescence intensity as a function of sample position along the optical axis. (**c**) Absorption coefficient of the 300 μM FAD sample. (**d**) Comparison of the predicted (——) and measured (■) peak fluorescence intensity as a function of sample position along the optical axis.

Figure 4a shows the spectra of each layer and the two-layer sample (with light incident on the Rhodamine 6G layer) obtained with the nonconfocal spectrometer. It is obvious that the spectrum of the two-layer sample contains contributions from both fluorophores; however, from these data it cannot be determined whether the sample consists of a single layer containing two homogeneously distributed fluorophores or multiple layers with different fluorophores. Furthermore, it is not possible to accurately determine flurophore concentrations from this spectrum without additional information about the sample geometry and optical properties. Note that the intensity due to FAD is considerably weaker in the spectrum of the two-layer sample than in the spectrum of the FAD layer alone. This result occurs both because of attenuation of the excitation and emitted light by the Rhodamine 6G layer and because the FAD layer was slightly behind the focal point of the spectrometer. Figures 4b–4d, which show spectra of the two-layer sample as the focal point of the confocal system was translated through the sample, illustrate the advantages of the confocal system. Here, spectra from the initial 1.5 mm (Fig. 4b) of the sample clearly contain contributions only from the Rhodamine 6G. At the interface between the layers (Fig. 4c), the spectra of both Rhodamine 6G and FAD are visible, and in the second layer (Fig. 4d) only FAD contributes. The thickness of the front layer can also be determined from these measurements. The ratio of fluorescence intensity at 540 to 580 nm is very different for Rhodamine 6G (0.07) and FAD (1.5); thus, by plotting this ratio as a function of sample position along the optical axis, one can measure the layer thickness. As shown in Fig. 4e, this value is nearly constant on either side of a transition region occurring 1.6 mm from the sample front face. This result agrees well with the measured layer thickness of 1.58 mm. These data also provide information about the attenuation coefficient of each layer at the excitation and emission wavelengths. Figure 4b shows that the fluorescence intensity detected from the Rhodamine 6G layer is relatively constant as the focal point is translated deeper within the sample, while the intensity recorded from the FAD layer decreases rapidly (Fig. 4d). The shape of the emission spectra remains constant in each case. This observation indicates that the absorption coefficient of each layer is constant over the emission wavelength region and that the sum of the absorption coefficients at the excitation and emission wavelengths is much greater in the FAD layer than in the Rhodamine 6G layer. This result is consistent with the measured absorption coefficients of each layer shown in Fig. 4f. If we assume that each layer

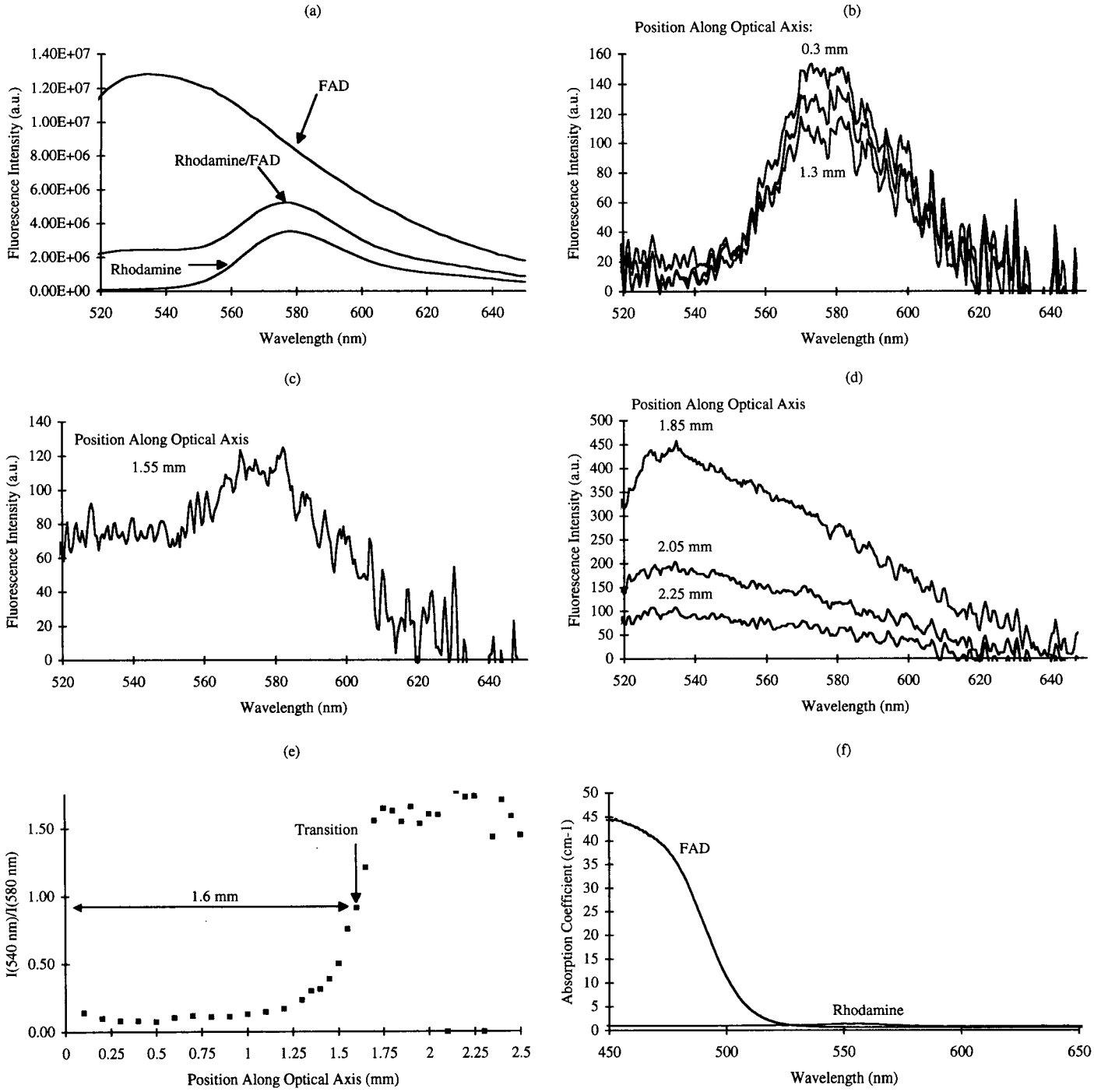

FIG. 4. (a) Fluorescence emission spectra obtained with a nonconfocal fluorimeter from individual Rhodamine 6G and FAD gelatin layers and the two-layer specimen with light incident on the Rhodamine 6G layer. (b) Confocal fluorescence spectra of the two-layer sample as the focal point of the system was translated past the sample front face and through the layer containing Rhodamine 6G. (c) Confocal fluorescence spectra of the two-layer sample with the focal point near the interface between the two layers. (d) Confocal fluorescence spectra of the two-layer sample as the focal point was translated through the second layer containing FAD. (e) Ratio of fluorescence intensity at 540 nm to that at 580 nm as a function of sample position along the optical axis. (f) Absorption coefficients of the individual gelatin layers.

is homogeneous, Eq. 3 can be used to estimate the sum of the absorption coefficients at the excitation and emission wavelength within each layer. If each layer contains only a single fluorophore, then this approach can be used to calculate fluorophore concentration. Thus, the confocal measurements readily provide information about the sample geometry and optical properties not available from nonconfocal measurements.

CONCLUSIONS

A fiber-optic confocal spectrometer which is inexpensive and easy to construct and to interface to existing spectrometers has been demonstrated. Depth-resolved, attenuated, fluorescence emission spectra measured with this confocal system provide information about the composition and optical properties of homogeneous and in-

homogeneous samples unavailable from conventional (nonconfocal) spectroscopic methods. Although only confocal fluorescence spectra were presented, the optical system described here can also be used, in principle, to acquire depth-resolved attenuated reflectance spectra by replacing the excitation source with white light illumination.

The demonstrated advantages of the confocal system indicate that it may be useful in characterizing the depth-resolved attenuated spectra of human tissues, where information about the variation in tissue structure with depth is of clinical importance. In particular, the optics of the current system would permit studies of easily accessible sites such as skin, oral mucosa, and cervical epithelium. Replacing the microscope objectives which deliver excitation light to and collect emitted light from the sample with graded index lenses may enable interrogation of other mucosal organs such as the colon and urinary bladder via endoscopes.

ACKNOWLEDGMENT

This work was supported by a grant from the National Science Foundation, No. BCS-9253612.

1. R. R. Alfano, A. Pradhan, and G. C. Tang, J. Opt. Soc. Am. B **6,** 1015 (1989).
2. R. R. Richards-Kortum, R. Rava, M. Fitzmaurice, L. Tong, N. B. Ratliff, J. R. Kramer, and M. S. Feld, IEEE Trans. Biomed. Eng. **36,** 1222 (1989).
3. R. M. Cothren, R. R. Richards-Kortum, M. V. Sivak, M. Fitzmaurice, R. P. Rava, G. A. Boyce, G. B. Hayes, M. Doxtader, R. Blackman, T. Ivanc, M. S. Feld, and R. E. Petras, Gastrointest. Endosc. **36,** 105 (1990).
4. K. Shomacker, J. Frisoli, C. C. Compton, T. Flotte, J. M. Richter, N. Nishioka, and T. Deutsch, Lasers Surg. Med. **12,** 63 (1992).
5. S. Lam, J. Y. C. Hung, S. M. Kennedy, J. C. Leriche, S. Vedal, B. Nelems, C. Macaulay, and B. Palcic, Am. Rev. Respir. Dis. **146,** 1458 (1992).
6. S. Andersson-Engels, J. Johansson, K. Svanberg, and S. Svanberg, Photochem. Photobiol. **53,** 807 (1991).
7. R. S. Cotran, V. Kumar, and S. L. Robbins, *Pathologic Basis of Disease* (W. B. Saunders Co., Philadelphia, 1989), 4th ed.
8. A. Durkin, S. Jaikumar, N. Ramanujam, and R. R. Richards-Kortum, Appl. Opt. (1993), paper in press.
9. J. Wu, M. S. Feld, and R. P. Rava, Appl. Opt. **32,** 3585 (1993).
10. C. Gardner, S. L. Jacques, and A. J. Welch, in *Proceedings of Advances in Fluorescence Sensing Technology,* SPIE Vol. 1885, J. R. Lakowicz and R. B. Thompson, Eds. (SPIE, Bellingham, Washington, 1993), pp. 122–128.
11. *Confocal Microscopy,* T. Wilson, Ed. (Academic Press, London, 1990).
12. K. P. Ghiggino, M. R. Harris, and P. G. Spizzirri, Rev. Sci. Instrum. **63,** 2999 (1992).
13. X. Gan, M. Gu, and C. J. R. Sheppard, J. Mod. Opt. **39,** 825 (1992).
14. S. Kimura and T. Wilson, Appl. Opt. **30,** 2143 (1991).
15. A. F. Gmitro and D. Aziz, Opt. Lett. **18,** 565 (1993).
16. G. J. Puppels, W. Colier, J. H. F. Olminkhof, C. Otto, F. F. M. de Mul, and J. Greve, J. Raman Spectrosc. **22,** 217 (1991).
17. G. J. Puppels, F. F. M. de Mul, C. Otto, J. Greve, M. Robert-Nicoud, D. J. Arndt-Jovin, and T. M. Jovin, Nature **347,** 301 (1991).
18. K. Sasaki, M. Koshioka, and H. Masuhara, Appl. Spectrosc. **45,** 1041 (1991).
19. J. Zeng, A. Durkin, and R. Richards-Kortum, in *Conferences on Lasers and Electro-Optics, 1993,* Vol. 11, OSA Technical Digest Series (Optical Society of America, Washington, D.C., 1993), pp. 98–99.
20. J. M. Khosrofian, Appl. Opt. **22,** 3406 (1983).
21. T. R. Corle, C. H. Chou, and G. S. Kino, Opt. Lett. **11,** 770 (1986).